To obtain the radiation field, (28) and (29) are substituted in (84), and the resulting integral is evaluated by the method of stationary phase for $k\rho \gg 1$. The result is

$$[H_y(x, z)]_R = \left(\frac{2}{\pi k\rho}\right)^{1/2} e^{i(k\rho-(\pi/4))} \cdot \frac{\tan \alpha_1}{(1 + \sec \alpha_1)^{1/2}} \frac{(1 + \cos \theta)^{1/2}}{(\cos^2 \theta - \sec^2 \alpha_1)} \cdot \quad (87)$$

The total power in the reflected surface wave per unit width of the screen is easily computed from (86), (74) and (76) as

$$P_r = 2 \int_0^\infty \hat{x} \cdot \boldsymbol{E}_r \times \boldsymbol{H}_r^* dz = \frac{2 \sin \alpha_1}{k(1 + \sec \alpha_1)^2} \cdot \quad (88)$$

The power radiated per unit width of the screen, per unit area in the direction $\theta$ is obtained from (87), (74), (76) and (28) when $k\rho \gg 1$ as

$$S = \text{Re}\, \hat{\rho} \cdot \boldsymbol{E}_R \times \boldsymbol{H}_R^* = \frac{2}{\pi k\rho} \frac{1}{(1 + \sec \alpha_1)} \frac{1 + \cos \theta}{(\sec^2 \alpha_1 - \cos^2 \theta)} \cdot \quad (89)$$

Hence, the total radiated power is

$$P_R = \int_0^{2\pi} S\rho d\theta = \frac{4}{k} \frac{1}{(1 + \sec \alpha_1)} \frac{\cos \alpha_1}{\tan \alpha_1} \cdot \quad (90)$$

It is to be noted that $P_r + P_R$ is equal to $P_i$ as given in (35). The power reflection coefficient and the radiation pattern are noticed to be the same with or without the terminating perfectly conducting half-plane.


## Acknowledgment

The author wishes to thank Prof. R. W. P. King and Tai Tsun Wu for their help and encouragement with this research.


# Surface Waves on Radially Inhomogeneous Cylinders*

A. VIGANTS†, MEMBER, IRE, AND S. P. SCHLESINGER†, MEMBER, IRE

*Summary*—**A characteristic equation and a cutoff equation are derived for higher order surface-wave modes on lossless isotropic cylinders with arbitrary radial permittivity variation. The derivation, based on the use of the fundamental matrix of a set of differential equations, reduces analytical work and results in expressions well suited for digital computer evaluation of surface-wave eigenvalues and mode spectra. The theory is applied in an investigation of $HE_{21}$ and $EH_{21}$ mode propagation for a particular set of models for the radially varying permittivity. Typical results showing eigenvalue variation, dispersion characteristics and radial field variation, including experimental verification of dispersion characteristics, are shown. The method of analysis can be extended to anisotropic cylinders with permittivity a function of both radius and frequency.**

## Introduction

THIS PAPER is concerned with the problem of surface-wave propagation along lossless isotropic cylinders with radial permittivity variation. The permittivity variation may be described by a function of the radius or an experimental curve, with discontinuities allowed. Step permittivity variation, such as that created by dielectric rods and tubes made of constant permittivity material,[1,2] constitutes a special case of the problem.

Electromagnetic-wave propagation along cylindrical structures inhomogeneous in the transverse plane has been investigated by Adler.[3,4] Some basic results about orthogonality, power flow and phase constants are obtained but the general problem of formulating the differential equations and obtaining their solutions is not considered. An interesting way to formulate differential equations for fields in inhomogeneous media has been proposed by Smith.[5] The approach is based on a transformation which contains the space dependent permittivity. This involves work with quantities other than electromagnetic fields and may not be desirable in a

* Received February 16, 1962; revised manuscript received May 31, 1962. This research was supported by the Air Force Cambridge Research Laboratories under Contract No. AF 19(604)3879.

† Department of Electrical Engineering, Columbia University, New York, N. Y.

[1] P. Diament, S. P. Schlesinger, and A. Vigants, "A dielectric surface wave structure: the V-line," IRE TRANS. ON MICROWAVE THEORY AND TECHNIQUES, vol. MTT-9, pp. 332–337; July, 1961.

[2] E. Snitzer, "Cylindrical waveguide modes," *J. Opt. Soc. Am.*, vol. 51, pp. 491–498; May, 1961.

[3] R. B. Adler, "Properties of Guided Waves on Inhomogeneous Cylindrical Structures," Electronics Res. Lab., M.I.T., Cambridge, Mass., Tech. Rept. No. 102; May 27, 1949.

[4] R. B. Adler, "Waves on inhomogeneous cylindrical structures," PROC. IRE, vol. 40, pp. 339–348; March, 1952.

[5] P. D. P. Smith, "Artificial field equations for a region where $\mu$ and $\epsilon$ vary with position," *J. Appl. Phys.*, vol. 21, pp. 1140–1149; November, 1950.

complicated surface-wave problem. Considerable insight into the problems of formulation of differential equations for electromagnetic fields in inhomogeneous media is obtained from Nisbet's work.[6] A result of particular interest is a set of conditions relating the order of the differential equations to the coordinate system and the functional dependence of the inhomogeneities. Application of these conditions to the radially inhomogeneous cylindrical medium shows that differential equations of higher order than the second can be expected.

A convenient general approach for the determination of inhomogeneous cylinder propagation characteristics does not appear to be available. In view of this it seems advisable to disregard the complicated methods of generation of differential equations while searching for a way to solve the radially inhomogeneous cylinder problem and to use Maxwell's equations directly,[7,8] thus avoiding confusion of physical intuition by complicated and possibly unnecessary mathematical devices.

The complexity of the inhomogeneous cylinder problem is due to differential equations of the fourth order with variable coefficients and a geometry which makes it difficult to use expansions in series of known functions. The radial variation of fields inside the inhomogeneous cylinder will in general be given by untabulated and unknown functions, and hence computation will be required to find the parameters characterizing surface-wave propagation. Realization of this leads to the formulation of a characteristic equation based on the application of the *fundamental matrix* of a set of differential equations, unusual in the solution of surface wave problems.

The results are applied in an investigation of $HE_{21}$ and $EH_{21}$ modes for a particular set of permittivity models, with experimental verification in some cases.

## Theory

### *The Characteristic and Cutoff Equations*

The lossless, isotropic, radially inhomogeneous cylinder shown in Fig. 1 presents a boundary value problem with solutions characterized by eigenvalues of a characteristic equation. Formulation of the boundary value problem requires knowledge of solutions inside the cylinder. The separation of variables technique applied to Maxwell's equations shows that solutions of the form $\exp in\phi$ for the circumferential variation of fields are

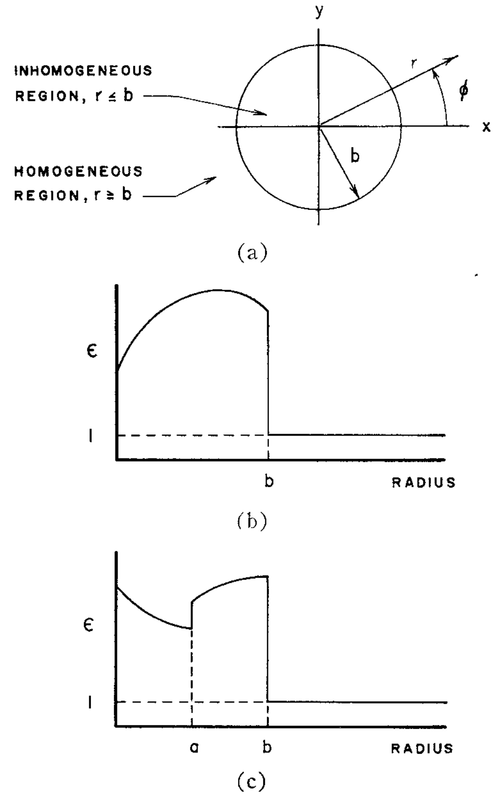


Fig. 1—The radially inhomogeneous cylinder surrounded by free space. (a) Geometry. (b) Example of permittivity variation without discontinuities in the inhomogeneous region. (c) Example of permittivity variation with a discontinuity in the inhomogeneous region.

permissible in a cylindrical medium with radial permittivity variation. This is the same result as that arrived at by physical reasoning—taking the case of continuous radial variation as the limiting case for a set of homogeneous shells. Therefore the postulated surface-wave mode fields inside the cylinder can be expressed as functions of radius multiplied by $\exp i(\omega t - n\phi - \beta z)$ where $\omega$ is the radian frequency and $\beta$ the phase constant of a surface-wave mode. The solutions in the homogeneous outside medium are of the same form.[9] Since the circumferential variation inside and outside the cylinder can be described by the same set of functions, the characteristic equation can be formulated for a single term in the solution, or mode, as is done in the case of a homogeneous cylinder.[9] This will now be done taking $n$ as an integer larger than one since the modes of interest in this work are higher order modes on full cylinders.

The fields occurring in the formulation of the boundary value problem are expressed as unknown functions of radius multiplied by $\exp i(\omega t - n\phi - \beta z)$. The unknown radial variations are expressed in a particular form, normalized radius raised to a power multiplied by an unknown function of the radius, in order to simplify the

[6] A. Nisbet, "Electromagnetic potentials in a heterogeneous non-conducting medium," *Proc. Roy. Soc.* (*London*) A, vol. 240, pp. 375–381; 1957.

[7] A. Vigants, "Propagation of Electromagnetic Surface Waves along Cylindrical Columns with Arbitrary Radial Permittivity Variation," Dept. of Elec. Engrg., Columbia University, New York, N. Y., Tech. Rept. No. 69, AF 19(604)3879; August 31, 1961.

[8] A. Vigants and S. P. Schlesinger, "Some Results on Electromagnetic Surface Wave Propagation Along Inhomogeneous Cylinders," Dept. of Elec. Engrg., Columbia University, New York, N. Y., Tech. Rept. No. 70, AF 19(604)3879; January 10, 1962.

[9] S. A. Schelkunoff, "Electromagnetic Waves," D. Van Nostrand Company, Inc., New York, N. Y., pp. 425–428; 1943.

algebra in subsequent expressions. The specific expressions are

$$\begin{aligned} E_z(r,\phi,z,t) &= x^n f_1(x)\exp i(\omega t - n\phi - \beta z)\\ E_\phi(r,\phi,z,t) &= x^{n-1} f_2(x)\exp i(\omega t - n\phi - \beta z)\\ H_z(r,\phi,z,t) &= i\eta_0^{-1}x^n f_3(x)\exp i(\omega t - n\phi - \beta z)\\ H_\phi(r,\phi,z,t) &= i\eta_0^{-1}x^{n-1} f_4(x)\exp i(\omega t - n\phi - \beta z) \end{aligned} \tag{1}$$

where

$$\begin{aligned} x &= kr\\ k^2 &= \omega^2\mu_0\epsilon_0 = (2\pi/\lambda_0)^2\\ \eta_0 &= (\mu_0/\epsilon_0)^{1/2}. \end{aligned} \tag{2}$$

The differential equations for the unknown functions of the radius are obtained by using (1) in Maxwell's equations. This results in a fourth-order system of ordinary differential equations with variable coeffcients

$$(d/dx)\boldsymbol{F}(x) = \boldsymbol{A}(x)\boldsymbol{F}(x) \tag{3}$$

where

$$\boldsymbol{F}(x) = \begin{bmatrix} f_1(x)\\ f_2(x)\\ f_3(x)\\ f_4(x)\end{bmatrix}. \tag{4}$$

The order of the system of differential equations reflects the coupling of the fields due to the permittivity variation and agrees with that obtained using Hertz potentials[6] or the separation of variables technique.

The description of the medium is contained in the coefficient matrix of the differential equation

$$\boldsymbol{A}(x) = \frac{1}{x}\begin{bmatrix} -n & 0 & -nU/\epsilon & -(\epsilon - U^2)/\epsilon\\ 0 & -n & (\epsilon x^2 - n^2)/\epsilon & nU/\epsilon\\ -nU & -(\epsilon - U^2) & -n & 0\\ (\epsilon x^2 - n^2) & nU & 0 & -n \end{bmatrix}$$

$$U = \beta/k \tag{5}$$

where $\epsilon$ is the relative permittivity, a function of the normalized radius. It can be shown that as $x$ approaches zero as the center of the cylinder is approached, (3) has a nonsingular solution which tends towards a constant. Hence a physically significant initial value for $\boldsymbol{F}(x)$ is

$$\boldsymbol{F}(0) = \text{constant}. \tag{6}$$

This means, from (1), that fields near the axis of the cylinder vary as $x^n$ and $x^{n-1}$. This agrees with physical reasoning since in the homogeneous case[9] the Bessel functions give a field variation as $x^n$ and $x^{n-1}$ near the axis of the cylinder. Investigation of $\boldsymbol{A}(0)$ shows that there are only two independent constants in $\boldsymbol{F}(0)$. A convenient way to express $\boldsymbol{F}(0)$, using $\boldsymbol{A}(0)$, is

$$\begin{aligned} f_1(0) &= n^{-1}(UB - D)\\ f_2(0) &= B\\ f_3(0) &= -n^{-1}[\epsilon(0)B - UD]\\ f_4(0) &= D \end{aligned} \tag{7}$$

where $B$ and $D$ are field magnitude constants.

A basic requirement of the boundary value problem formulation is that the solution in the inhomogeneous medium be expressed in a form which is convenient in the solution of the characteristic equation. In particular the requirement is for expressions which simplify both analytical work and digital computer evaluation of the characteristic equation. This can be achieved by expressing the solution of (3) as

$$\boldsymbol{F}(x) = \boldsymbol{B}(x, 0)\boldsymbol{F}(0) \tag{8}$$

where $\boldsymbol{B}(x, 0)$ is the *fundamental matrix* for (3). The properties and construction of fundamental matrices are part of the theory of differential equations.[10] If $\boldsymbol{A}(x)$ is known then $\boldsymbol{B}(x, 0)$ can be computed; one way of doing it is outlined in the Appendix.

The value of $\boldsymbol{F}(x)$ on the boundary, approached from the inhomogeneous region, expressed in terms of $\boldsymbol{F}(0)$ is

$$\boldsymbol{F}(kb^-) = \boldsymbol{B}(kb^-, 0)\boldsymbol{F}(0). \tag{9}$$

If there is a discontinuity such as shown in Fig. 1(c), then

$$\boldsymbol{B}(kb^-, 0) = \boldsymbol{B}(kb^-, ka^+)\boldsymbol{B}(ka^-, 0) \tag{10}$$

since $\boldsymbol{F}(x)$ is continuous across discontinuities in permittivity. Hence discontinuities are taken care of by cascading fundamental matrices for the different regions. Because of the continuity of $\boldsymbol{F}(x)$ the boundary condition is simply

$$\boldsymbol{F}(kb^+) = \boldsymbol{F}(kb^-) \tag{11}$$

or using (9)

$$\boldsymbol{F}(kb^+) = \boldsymbol{B}(kb^-, 0)\boldsymbol{F}(0) \tag{12}$$

where $\boldsymbol{F}(kb^+)$, the value on the boundary approached from outside, is given by appropriate homogeneous medium solutions.[9]

$$\begin{aligned} f_1(kb^+) &= (kb)^{-n}\{MK_n(q)\}\\ f_2(kb^+) &= (kb)^{-n}\{q/2(1-U^2)\}\{N[K_{n-1}(q) + K_{n+1}(q)]\\ &\qquad + MU[K_{n-1}(q) - K_{n+1}(q)]\}\\ f_3(kb^+) &= (kb)^{-n}\{NK_n(q)\}\\ f_4(kb^+) &= (kb)^{-n}\{q/2(1-U^2)\}\{M[K_{n-1}(q) + K_{n+1}(q)]\\ &\qquad + NU[K_{n-1}(q) - K_{n+1}(q)]\}. \end{aligned} \tag{13}$$

[10] E. A. Coddington and N. Levinson, "Theory of Ordinary Differential Equations," McGraw-Hill Book Company, Inc., New York, N. Y., pp. 67–74; 1955.

There are two field magnitude constants, $M$ and $N$, contained in the left-hand side of (12). The right-hand side contains two other field magnitude constants, $B$ and $D$, in $\boldsymbol{F}(0)$. The description of the inhomogeneous medium is contained in $\boldsymbol{B}(kb^-, 0)$.

The characteristic equation is obtained by arranging the terms of (12) in the form

$$\mathbf{C}\begin{bmatrix} B \\ D \\ M \\ N \end{bmatrix} = 0 \tag{14}$$

which gives the characteristic equation

$$\det \mathbf{C} = 0 \tag{15}$$

since the field magnitudes must be nonzero. The elements of the determinant are

$$c_{i1} = b_{i1}n^{-1}U + b_{i2} - b_{i3}n^{-1}\epsilon(0)$$

$$c_{i2} = -b_{i1}n^{-1} + b_{i3}n^{-1}U + b_{i4}$$

$$i = 1, 2, 3, 4$$

$$c_{13} = c_{34} = -(kb)^n K_n(q)$$

$$c_{23} = c_{44} = \frac{(kb)^{2-n}}{2q} U[K_{n-1}(q) - K_{n+1}(q)]$$

$$c_{33} = c_{14} = 0$$

$$c_{43} = c_{24} = \frac{(kb)^{2-n}}{2q} [K_{n-1}(q) + K_{n+1}(q)] \tag{16}$$

with the first two columns of $\mathbf{C}$ describing the inhomogeneous medium and the last two the homogeneous bounding medium. The $b_{ij}$ are elements of the fundamental matrix $\boldsymbol{B}(kb^-, 0)$.

The characteristic equation yields eigenvalue pairs $(q, kb)$ which characterize surface-wave modes on radially inhomogeneous cylinders. The quantity $q$ is a radial eigenvalue for the fields outside the cylinder.[9]

For a given surface-wave mode there is a frequency below which this mode does not exist. This is labeled "cutoff" frequency in surface-wave terminology. At cutoff

$$U = \beta/k = 1 \tag{17}$$

which implies from[9]

$$(q/kb)^2 = U^2 - 1 \tag{18}$$

that $q$ is zero if $kb$ is finite and nonzero. An assumption can be made, based on physical reasoning and homogeneous cylinder cutoff expressions, that $kb$ will be finite and nonzero for the higher order modes considered in this work.

As $q$ approaches zero some elements in (16) become singular and algebraic manipulation is necessary.[7] To obtain the cutoff equation $K_{n+1}(q)$ is eliminated using recursion formulas. For small $q$

$$\lim_{q\to 0} K_{n-1}(q)/qK_n(q) = 1/2(n-1). \tag{19}$$

When this is used the dominant term in the characteristic equation is that containing $q^{-2}$. The coefficient of this term gives the cutoff equation

$$\lim_{U\to 1} \left\{ (c_{11} - c_{31})(c_{22} + c_{42}) + (c_{21} + c_{41})(c_{32} - c_{12}) + \left[\frac{(kb)^2}{n-1} - n\right](c_{11}c_{32} - c_{31}c_{12}) \right\} = 0. \tag{20}$$

The unknown quantity in this equation is the cutoff value of $kb$.

It is interesting to note that a single equation gives cutoff values for all higher order modes as opposed to a set of two equations for homogeneous cylinders.[1,2]

*Designation of Solutions*

The inhomogeneous cylinder problem is a generalization of the homogeneous cylinder problem. To avoid confusion in borderline cases the system of mode designations for the inhomogeneous cylinder will be identical with that for the homogeneous cylinder. Specifically, homogeneous cylinder solutions are characterized by $(p, q)$ pairs[1] with corresponding $(q, kb)$ pairs obtained from the expression

$$p^2 + q^2 = (\epsilon - 1)(kb)^2$$
$$\epsilon = \text{const.} \tag{21}$$

The system[1,2] used for classifying homogeneous cylinder modes can be summarized as follows for $n$ larger than one. For a given $n$ and $q$ the $(q, kb)$ pairs are ordered according to the magnitude of $kb$, starting with the pair containing the lowest value of $kb$. The solution corresponding to the first $(q, kb)$ pair is called the $\text{HE}_{n1}$ mode. The sequence of mode designations for solutions corresponding to the subsequent $(q, kb)$ pairs is $\text{EH}_{n1}$, $\text{HE}_{n2}$, $\text{EH}_{n2}$, $\text{HE}_{n3}$, etc. The confusing situation of two modes with the same subscripts, $\text{HE}_{nm}$ and $\text{EH}_{nm}$, is the result of investigations[11] to determine which of the field components, electric or magnetic, in the direction of propagation contributes more to certain other field components. For inhomogeneous cylinders the eigenvalue pairs $(q, kb)$ will be ordered and mode designations assigned to this sequence as described for the homogeneous case.

## Some Results

The characteristic equation and the cutoff equation were used to determine $\text{HE}_{21}$ and $\text{EH}_{21}$ mode parameters for permittivity models represented by the first three

[11] R. E. Beam, M. M. Astrahan, W. C. Jakes, H. H. Wachowski, and W. L. Firestone, "Investigations of Multimode Propagation in Waveguides and Microwave Optics," Microwave Lab., Northwestern University, Evanston, Ill., Rept. ATI 94929, ch 5; 1949.

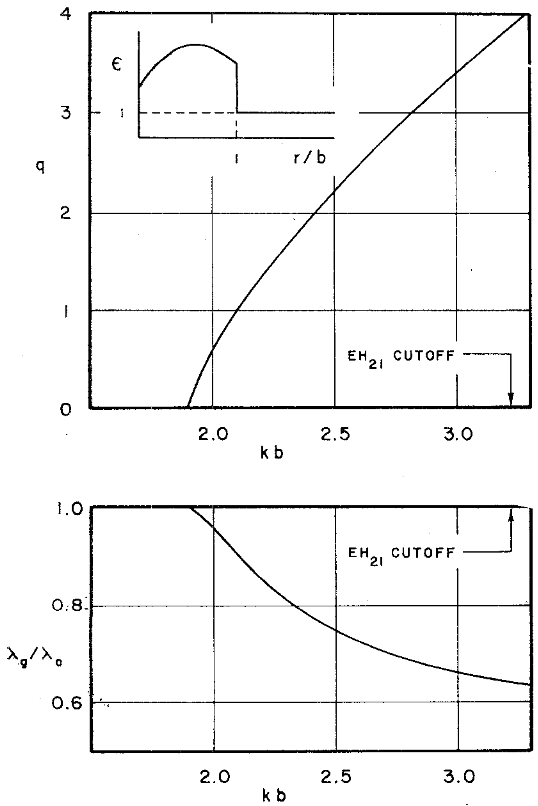


Fig. 2—$HE_{21}$ mode parameters for the permittivity variation $\epsilon=2+6(r/b)-5(r/b)^2$, $0\leq r\leq b$.

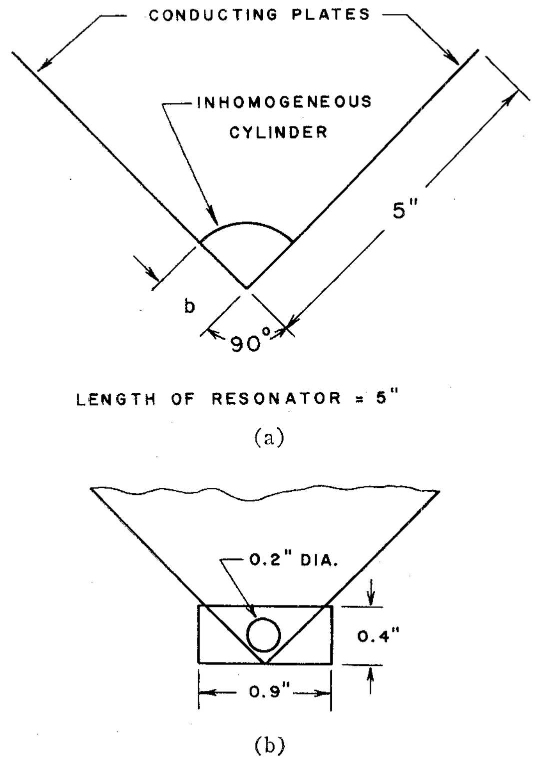


Fig. 4—The surface wave resonator. (a) Cross section. (b) Sketch of coupling hole between end of $x$-band waveguide and surface wave resonator end plate. The rectangular waveguide is excited in the $TE_{10}$ mode.

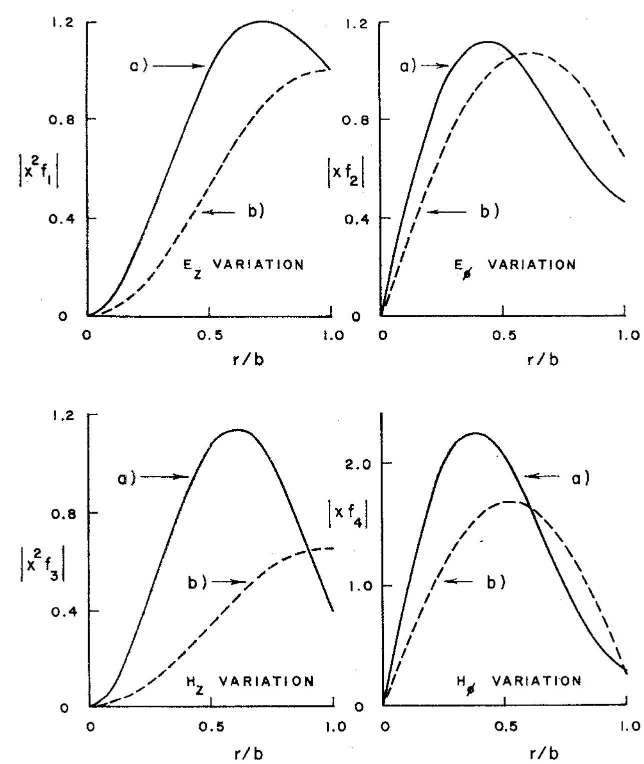


Fig. 3—Radial variation of electromagnetic fields for the $HE_{21}$ mode. a) $\epsilon=4-3(r/b)^2$, $0\leq r\leq b$, $q=1.85$, $kb=2.964$. b) $\epsilon=2.56$, $0\leq r\leq b$, $q=1.85$, $kb=2.949$.

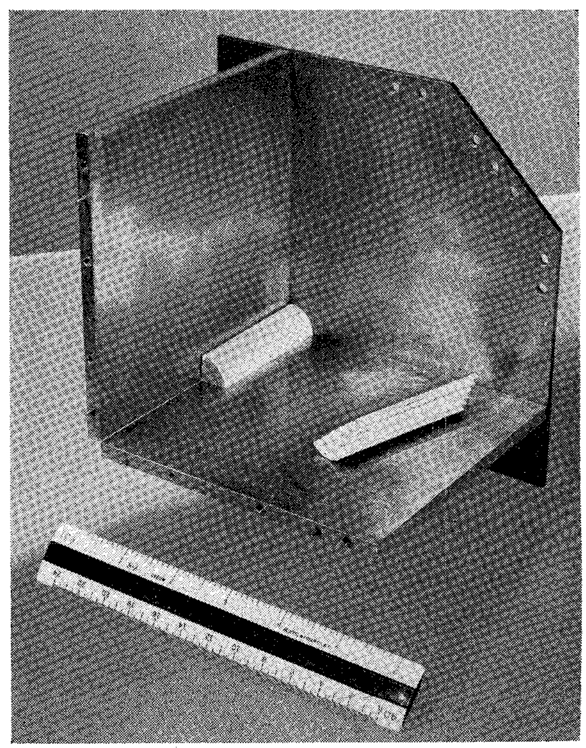

Fig. 5—Photograph of surface wave resonator with one end plate removed, showing half of an inhomogeneous six-layer experimental permittivity model in place in the cavity. The other half of the permittivity model is displayed near the edge of the cavity.

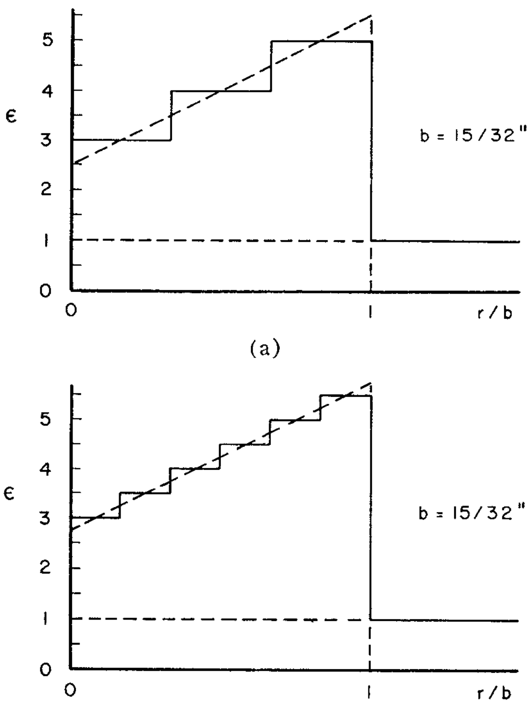


Fig. 6—Experimental permittivity models with positive slopes. (a) Experimental three-step approximation of the theoretical variation $\epsilon=2.50+3(r/b)$, $0\leq r\leq b$. (b) Experimental six-step approximation of the theoretical variation $\epsilon=2.75+3(r/b)$, $0\leq r\leq b$.

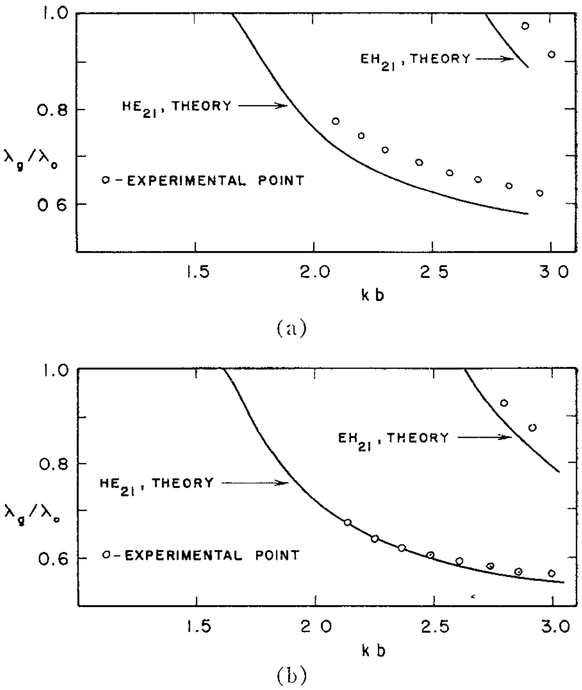


Fig. 8—Experimental verification of theory using permittivity models with positive slopes shown in Fig. 5. (a) Theoretical data for $\epsilon=2.50+3(r/b)$, $0\leq r\leq b$ and experimental data for the corresponding three-step approximation of the theoretical model. (b) Theoretical data for $\epsilon=2.75+3(r/b)$, $0\leq r\leq b$ and experimental data for the corresponding six-step approximation of the theoretical model.

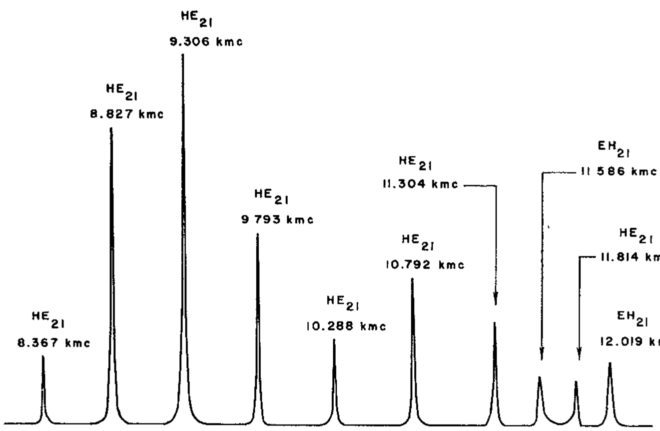


Fig. 7—Recorder plot of cavity resonances sensed with a probe for the experimental three-step permittivity variation shown in Fig. 6(a).

terms of a power series in $(r/b)$.

$$\begin{aligned} \epsilon &= d_1 + d_2(r/b) + d_3(r/b)^2 \qquad & r \leq b \\ &= 1 & r \geq b. \end{aligned} \tag{22}$$

Propagation characteristics of a number of permittivity models of interest to the authors were determined[7,8]. A typical set of characteristics is shown in Fig. 2. The general shapes of the characteristics are similar to those of homogeneous cylinders[1].

The radial variation of electromagnetic fields in the inhomogeneous cylinder is of interest because the functions representing the variations are untabulated. The radial variation of fields can be computed once the eigenvalues are known by first using (14) to find the field magnitude constants and then using (8). Examples were considered where an inhomogeneous and a homogeneous cylinder have the same eigenvalue pair $(q, kb)$. Under these conditions guide wavelength measurements alone would not suffice to distinguish between the two cylinders. The data for two such cylinders are shown in Fig. 3. To simplify comparison the electric field $z$-component magnitudes have been normalized to unity on the boundary. The eigenvalues are not exactly the same but differences of about one per cent in $kb$ will not affect the field drawings significantly. The results of Fig. 3 show that the radial variation of $E_z$ and $H_z$ is not described by the same function of radius, whereas in the homogeneous case the radial variation of $E_z$ and $H_z$ is given by the same Bessel function.

The theoretically predicted propagation characteristics were verified experimentally for two typical cases, using a surface-wave resonator and experimental permittivity models composed of homogeneous shells. The surface-wave resonator is shown in Figs. 4 and 5 and two experimental permittivity models are shown in Fig. 6. The cavity resonance plots for one of these are given in Fig. 7. The heights of the resonance peaks are not directly related to energy levels since for each resonance the sensing probe was at a different point of the standing wave in the cavity. The experimental and theoretical data are correlated in Fig. 8 with the conclusion that experimental points approach theoretical curves as the experimental models approach the theoretical models.

## Conclusion

The characteristic equation and the cutoff equation for higher order surface-wave modes on cylinders with arbitrary radial permittivity variation are derived in terms of the fundamental matrix of a set of differential equations. Some theoretical and experimental results are given for the $HE_{21}$ and $EH_{21}$ modes as an illustration.

The advantages of the fundamental matrix formulation of the inhomogeneous cylinder problem are compact analytic expressions and results which can be readily programmed for computation. The computation is not overly involved and hence the mode spectrum and properties can be obtained on a small computer such as an IBM 1620.

An extension of the ideas developed in this work to certain problems in plasmas[12–15] is possible since the method developed here can be modified to include a tensor permittivity which is a function of frequency and, rather important for a realistic approach, of the radius. Additional differential equations may be incorporated in the formulation. Under these conditions the possibility for analytical work afforded by the coefficient matrix of the system of first-order differential equations becomes important. This is a problem distinct from that discussed in this work, and a first application to it of the ideas developed in this work has given interesting results.

## Appendix

### *Empirical Cutoff Expressions*

The cutoff equation for inhomogeneous cylinders was formulated with digital computer solution in mind. In practical applications of the theory it is desirable, after the limits of permittivity variation are established, to have an expression for estimating cutoffs which does not require the use of a digital computer every time the permittivity model is changed. Such an expression can be derived by introducing the notion of an equivalent permittivity. As an illustration, $HE_{21}$ and $EH_{21}$ mode empirical cutoff relationships will be derived for the type of permittivity variation described in Table I.

The notion of an equivalent permittivity is introduced as follows: Let

$kb_c$ = cutoff value of $kb$

$\epsilon_{eq}$ = permittivity of a homogeneous cylinder which has the same $kb_c$ as the inhomogeneous cylinder.

[12] F. H. Northover, "The propagation of electromagnetic waves in ionized gases," IRE Trans. on Antennas and Propagation, *Special Supplement*, vol AP-7, pp. S340-S360; December, 1959.

[13] A. W. Trivelpiece and R. W. Gould, "Space charge waves in cylindrical plasma columns," *J. Appl. Phys.*, vol. 30, pp. 1748–1793; November, 1959.

[14] V. Bevc and T. E Everhart, "Fast Waves in Plasma Filled Waveguides," Electronics Res. Lab., University of California, Berkeley, Calif., Ser. No. 60, Issue No. 362, AF 19(616)6139; July 11, 1961.

[15] W. Van Tuyl Rusch, "Surface Waves on a Plasma Clad Cylinder," Elec. Engrg. Dept, University of Southern California, Los Angeles, Calif., Rept No. 82-202, AF 19(604)6195; September, 1961.

TABLE I

Permittivity Models for which $HE_{21}$ and $EH_{21}$ Mode Parameters were Computed[8]

| Model No. | Coefficients in (22) | | |
|---|---|---|---|
| | $d_1$ | $d_2$ | $d_3$ |
| 1 | 2.00 | 2.00 | 0 |
| 2 | 2.00 | 4.00 | 0 |
| 3 | 2.00 | 6.00 | 0 |
| 4 | 2.50 | 3.00 | 0 |
| 5 | 2.75 | 3.00 | 0 |
| 6 | 5.50 | −3.00 | 0 |
| 7 | 5.25 | −3.00 | 0 |
| 8 | 2.75 | 1.50 | 0 |
| 9 | 4.25 | −1.50 | 0 |
| 10 | 8.00 | −4.00 | 0 |
| 11 | 2.00 | 0 | 4.00 |
| 12 | 4.00 | 0 | −3.00 |
| 13 | 4.00 | 0 | 4.00 |
| 14 | 6.00 | 0 | 2.00 |
| 15 | 6.00 | 0 | −2.00 |
| 16 | 8.00 | 0 | −2.00 |
| 17 | 8.00 | 0 | −4.00 |
| 18 | 2.00 | 2.00 | 2.00 |
| 19 | 2.00 | 6.00 | −5.00 |
| 20 | 5.00 | −3.00 | 3.00 |
| 21 | 8.00 | −2.00 | −2.00 |

The average permittivity for (22) is

$$\epsilon_{av} = \int_0^1 \epsilon d(r/b) = d_1 + (d_2/2) + (d_3/3). \qquad (23)$$

It is assumed that for permittivity models within particular limits the equivalent permittivity can be expressed as a weighted average

$$\epsilon_{eq} = d_1 + w_2(d_2/2) + w_3(d_3/3) \qquad (24)$$

with weighting constants $w_1$ and $w_2$.

The weighting constants are found by solving the exact cutoff equation for $kb_c$ and using this value of $kb_c$ to determine the equivalent permittivity from homogeneous cylinder cutoff data[1] shown in Figs. 9 and 10. Then from permittivity models with $d_3$ equal to zero, see Table I,

$$w_2 = 2(\epsilon_{eq} - d_1)/d_2 \qquad (25)$$

and from models with $d_2$ equal to zero,

$$w_3 = 3(\epsilon_{eq} - d_1)/d_3. \qquad (26)$$

For the $HE_{21}$ mode and models listed in Table I the weighting constants fall between the limits

$$1.40 \leq w_2 \leq 1.50$$
$$1.65 \leq w_3 \leq 1.87 \qquad (27)$$

with averages

$$w_2 = 1.45$$
$$w_3 = 1.70 \qquad (28)$$

Hence an approximate expression for an equivalent permittivity for the $HE_{21}$ mode is justified

$$\epsilon_{eqHE21} \approx d_1 + 1.45(d_2/2) + 1.70(d_3/3). \qquad (29)$$

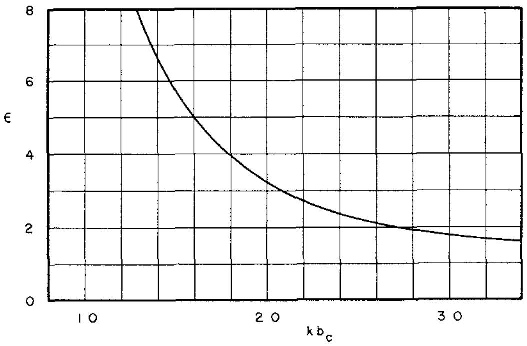


Fig. 9—Permittivity as a function of *kb* at cutoff for the $HE_{21}$ mode on homogeneous cylinders.

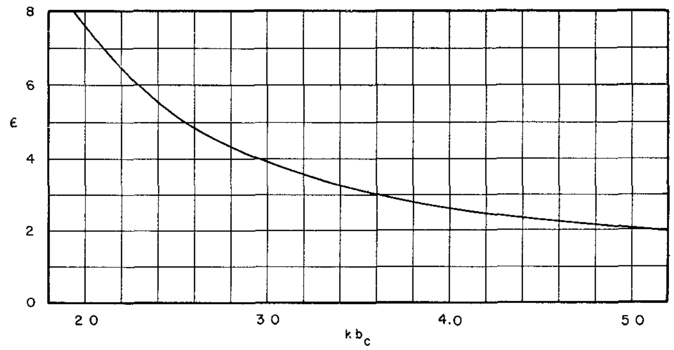


Fig. 10—Permittivity as a function of *kb* at cutoff for the $EH_{21}$ mode on homogeneous cylinders.

A similar derivation for the $EH_{21}$ mode gives

$$\epsilon_{\mathrm{eqEH}_{21}} \approx d_1 + 1.36(d_2/2) + 1.50(d_3/3) \qquad (30)$$

As an illustration of the usefulness of these approximate expressions consider the permittivity model

$$\begin{aligned} \epsilon &= 8 - 2(r/b) - 2(r/b)^2, & 0 \leq r \leq b \\ &= 1, & r \geq b \end{aligned} \qquad (31)$$

for which

$$\begin{aligned} \epsilon_{\mathrm{eqHE}_{21}} &\approx 5.45 \\ \epsilon_{\mathrm{eqEH}_{21}} &\approx 5.64 \end{aligned} \qquad (32)$$

and from Figs. 9 and 10

$$\begin{aligned} kb_{c\mathrm{HE}_{21}} &\approx 1.54 \\ kb_{c\mathrm{EH}_{21}} &\approx 2.37. \end{aligned} \qquad (33)$$

The digital computer results are

$$\begin{aligned} kb_{c\mathrm{HE}_{21}} &= 1.55 \\ kb_{c\mathrm{EH}_{21}} &= 2.41. \end{aligned} \qquad (34)$$

Time was saved by using the approximate expressions to predict initial values for digital computer work.

*Computation*

To express the fundamental matrix in a form convenient for computation the system of differential equations in (3) is replaced by a system of difference equations, with the order of the system retained to avoid instabilities.[16]

$$F_{m+1} = B_m F_m. \qquad (35)$$

This can also be written as

$$F_{m+1} = \prod_{i=0}^{m} B_i F_0 \qquad (36)$$

where by construction the $B_i$ product is a numerical approximation of the fundamental matrix of (3). The $B_m$ matrix in this work was obtained from $\boldsymbol{A}(x)$ by using a Runge-Kutta formula[17] correct through terms containing the computational increment to the third power.

$$\begin{aligned} B_m = I &+ (1/6)hA_m \\ &+ (4/6)(hA_{m+0.5} + 0.5h^2A_{m+0.5}A_m) \\ &+ (1/6)(hA_{m+1} + 2h^2A_{m+1}A_{m+0.5} \\ &+ h^3A_{m+1}A_{m+0.5}A_m - h^2A_{m+1}A_m) \end{aligned} \qquad (37)$$

where

$$\begin{aligned} I &= \text{unit matrix} \\ A_m &= \boldsymbol{A}(x_m) \\ h &= \text{increment in } x. \end{aligned} \qquad (38)$$

The elements of $A_0$ are singular, but since

$$A_0F_0 = 0 \qquad (39)$$

the elements of $A_0$ can be taken to be zero in the computation. For the models listed in Table I with

$$\begin{aligned} q &\leq 4 \\ h &= 0.1 \end{aligned} \qquad (40)$$

the accuracy, arrived at by considering special cases with known solutions, was about one per cent. Eigenvalues were computed on an IBM 1620 computer. The field variation was evaluated on an IBM 7090 computer.

[16] H. Rutishauser, "Über die Instabilität von Methoden zur Integration gewöhnlicher Differentialgleichungen," *Z. angew. Math. Phys.*, vol. 3, pp. 65–74; 1952.

[17] F. B. Hildebrand, "Introduction to Numerical Analysis," McGraw-Hill Book Company, Inc., New York, N. Y., p. 236; 1958.